


 Cite this: *Chem. Commun.*, 2024, 60, 1432

 Received 15th October 2023,  
Accepted 4th January 2024

DOI: 10.1039/d3cc05078e

rsc.li/chemcomm

# Covalent immobilization of N-heterocyclic carbenes on pristine carbon substrates: from nanoscale characterization to bulk catalysis†

 Brent Daelemans,<sup>ab</sup> Sven Bernaerts,<sup>a</sup> Samuel Eyley,<sup>c</sup> Wim Thielemans,<sup>c</sup> Wim Dehaen<sup>\*b</sup> and Steven De Feyter<sup>ab</sup>

**To control the synthesis of designer catalysts on graphitic materials up to the nanometer scale, methods should be provided that combine both nanoscale characterization and bulk scale experiments. This work reports the grafting of N-heterocyclic carbene (NHC)-type catalysts on graphite, both at nanometer and bulk scale, as it allows increased insights into the nature of the immobilized catalysts.**

Catalysis is at the core of industrial development with numerous applications in the chemical industry.<sup>1</sup> While the two main types of catalysts are heterogeneous and homogeneous catalysts, the production of immobilized catalysts is gaining more interest. Immobilized catalysts are able to combine the advantages of both heterogeneous (*i.e.* easy separation and recyclability) and homogeneous (*i.e.* high activity and selectivity) catalysts by immobilizing a homogeneous catalyst onto a solid surface.<sup>2–4</sup> A frequently used support is carbon owing to its mechanical stability, high surface area, and availability.<sup>3</sup> These carbon supports are often combined with N-heterocyclic carbene (NHC) moieties because of their versatile catalytic behavior.<sup>2–5</sup>

The bulk synthesis of these supported catalysts focuses on catalytic applications while the nature of the synthesized catalyst is often treated as being of minor importance. For this reason, highly functionalized and defective carbon substrates (*e.g.* graphene oxide) are used to achieve high catalyst loadings.<sup>6,7</sup> Disadvantages of this approach are a lack of insight into the grafting location of the catalytic moiety, as it is difficult to determine if the molecules graft on defects, on functional

groups, or on the basal plane.<sup>8–10</sup> Additionally, the presence of different functional groups could also contribute to the catalytic effect of the supported catalyst<sup>11</sup> and a transition towards more pristine carbon substrates would be beneficial.<sup>12,13</sup>

The minor importance allocated to the nature of the catalyst in bulk experiments is in shrill contrast with the control that can be obtained in nanoscale grafting experiments on highly oriented pyrolytic graphite (HOPG). The high-resolution on-surface characterization techniques available allow researchers to get a clear view on the nature of the functionalized carbon materials and to control the location,<sup>14</sup> the density,<sup>15</sup> the layer height,<sup>16</sup> and the removal of covalently attached molecules.<sup>17</sup> To achieve similar control over the functionalization of catalysts in bulk, grafting methods for catalysts that can be used on both nano- and bulk scale need to be developed.

This work provides a direct grafting method of a 1,2,4-triazolium NHC-precursor on both pristine HOPG and graphene nanoplatelets (GNP). In this way, HOPG can act as a model substrate to investigate the nature of the catalyst in bulk. The grafting method is then upscaled to GNP to increase its applicability in catalysis. Finally, the substrate is characterized and tested as an organocatalyst in benzoin condensation.

To allow covalent attachment to a graphitic substrate, a suitable NHC-precursor should be designed. In this aspect, a linker containing an aniline moiety was added. The aniline moiety can be converted to a diazonium group, which is commonly used in grafting experiments. The synthesis of the molecule starts from *N*-[4-(2-bromoethyl)phenyl]-acetamide (**1**) which was synthesized following an adaptation of a previously reported procedure.<sup>18,19</sup> Compound **1** was then reacted with 1-methyl-1,2,4-triazole to synthesize compound **2** and the amine group was deprotected to obtain product **3** (Scheme 1).<sup>20</sup> The 1,2,4-triazolium NHC catalyst was chosen because of its abundant use in benzoin condensation.<sup>5</sup> Additionally, compound **5** was synthesized to be used as a homogeneous catalyst for comparison with the supported catalyst.<sup>21</sup>

After the successful synthesis of the NHC precursor, grafting experiments were performed on HOPG to allow characterization

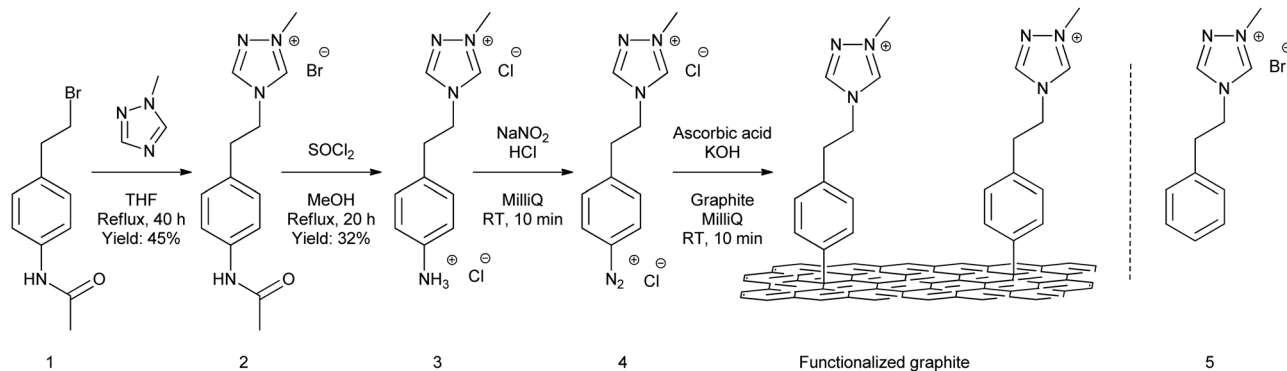
<sup>a</sup> Division of Molecular Imaging and Photonics, Department of Chemistry, KU Leuven, Celestijnenlaan 200F, Leuven 3001, Belgium. E-mail: steven.defeyter@kuleuven.be

<sup>b</sup> Division of Sustainable Chemistry for Metals and Molecules, Department of Chemistry, KU Leuven, Celestijnenlaan 200F, Leuven 3001, Belgium. E-mail: wim.dehaen@kuleuven.be

<sup>c</sup> Sustainable Materials Lab, Department of Chemical Engineering, KU Leuven, campus Kulak Kortrijk, E. Sabbelaan 53, Kortrijk 8500, Belgium

† Electronic supplementary information (ESI) available. See DOI: <https://doi.org/10.1039/d3cc05078e>





**Scheme 1** Synthesis of the triazolium NHC-precursor, followed by grafting of the NHC-precursor to a graphite substrate using chemical activation. Compound **5** will be used as a homogeneous catalyst for comparison.

with a broad range of surface characterization techniques. In these experiments, HOPG is considered a model substrate for bulk graphitic materials. To graft the molecule, chemical activation of the diazonium salt was preferred over electrochemical activation as this method can be scaled up to graphitic powders. Furthermore, our group recently reported a chemical activation method using ascorbic acid, which allowed us to gain more control over the functionalization by limiting the growth of the grafted layer to monolayers.<sup>15</sup> In this method, the ammonium salt **3** is converted to the diazonium salt **4** using  $\text{NaNO}_2$  and  $\text{HCl}$ . The success of the conversion to the diazonium salt was verified by repeating the reaction in  $\text{D}_2\text{O}$ , followed by characterization with  $^1\text{H-NMR}$  (Fig. S16, ESI<sup>†</sup>). Next, the method uses sequential drop-casting of an ascorbic acid/KOH solution and the diazonium salt solution on HOPG, which covalently binds the NHC-precursors to the graphite basal plane (Scheme 1). We refer to ref. 15 for a profound explanation of the mechanism. The functionalized substrate is then rinsed with acetonitrile and MilliQ water and dried. Afterwards, the functionalized HOPG substrate is characterized using different on-surface characterization techniques.

To get a clear description of the molecules attached to the surface, three different on-surface characterization techniques were performed: Raman spectroscopy, atomic force microscopy (AFM), and scanning tunneling microscopy (STM). From these techniques, Raman spectroscopy allows one to study the amount and the nature of the defects in a graphitic substrate.<sup>22,23</sup> For graphitic materials, the main bands that are considered are the G band, which is characteristic of the  $\text{sp}^2$  carbons, and the D band, which is induced by the presence of defects. For covalently functionalized materials, the amount of defects generally increases due to the conversion of  $\text{sp}^2$  carbons to  $\text{sp}^3$  carbons in the grafting process. The insertion of defects can be observed by the presence of a D band in the Raman spectrum (Fig. 1a), which is not observable for pristine HOPG (Fig. S5, ESI<sup>†</sup>), and the corresponding increase in the  $I_D/I_G$  ratio to  $0.041 \pm 0.007$ .

Atomic force microscopy (AFM) is a scanning probe microscopy technique that allows one to visualize the topography of the functionalized HOPG substrate at the air/solid interface. For the covalently functionalized HOPG sample, a granular structure is observed instead of a uniform HOPG surface which is attributed

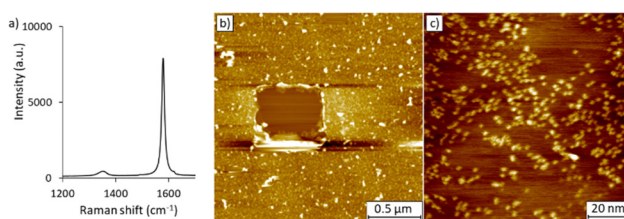


**Fig. 1** On-surface characterization of a HOPG substrate functionalized with the covalently bound triazolium: (a) Raman spectrum, (b) an AFM height image of  $2 \times 2 \mu\text{m}$  with a small area ( $0.5 \times 0.5 \mu\text{m}$ ) scratched away and (c) an STM image:  $100 \times 100 \text{ nm}$ ,  $I_{\text{set}} = 0.030 \text{ nA}$ ,  $V_{\text{bias}} = -0.900 \text{ V}$  are shown.

to the presence of grafted species (Fig. S1, ESI<sup>†</sup>).<sup>15</sup> Additionally, AFM provides more information on the height of the grafted layer *via* scratching experiments in which a part of the grafted layer is scratched away with the AFM tip to obtain the bare HOPG surface (Fig. 1b). When the height of the bare surface is compared to the adjacent grafted layer, the height of the grafted molecules can be calculated. For the functionalized substrate, the height of the grafted layer is  $2.7 \pm 0.4 \text{ nm}$ . Our molecule is expected to have a height of  $\pm 1.2 \text{ nm}$ , given that the height of an orthogonally grafted aryl group is  $\sim 0.8 \text{ nm}$ .<sup>15</sup> The observation thus suggests the formation of a bilayer, instead of a monolayer, which could be caused by the elimination of the triazolium group and reaction of a second molecule **3** with the polystyrene unit (Scheme S1, ESI<sup>†</sup>). Moreover, AFM was combined with infrared (IR) spectroscopy in which the characteristic peaks of the triazolium unit could be observed on the HOPG substrate (Fig. S2, ESI<sup>†</sup>).

To observe the individual species on the surface, high-resolution STM can be used (Fig. 1c). The covalently grafted species are observed as bright dots in the STM image, whereas no contrast differences are observed on a blank HOPG sample (Fig. S3, ESI<sup>†</sup>).<sup>15</sup> Furthermore, these molecules remain at the same spot during consecutive scans, which emphasizes their anchored nature (Fig. S4, ESI<sup>†</sup>).

To scale up from HOPG to graphitic powders, high surface area graphene nanoplatelets (GNP) were taken to allow a significant number of molecules to graft on the surface. GNP is expected to have a similar behaviour in grafting experiments



to the model substrate HOPG. However, in comparison to pristine HOPG, oxygen functionalities will be present in GNP which can react with the formed diazonium species. To limit these side reactions, low-defect high-surface area graphene derivatives should be prepared and used in the future. A similar covalent functionalization procedure as on HOPG, with ascorbic acid to chemically activate the diazonium salt, was performed. However, the functionalization procedure was altered slightly as a higher amount of surface area was used in bulk and the functionalization time was changed to 24 hours instead of 10 minutes. Due to the unsuitability of SPM techniques for the characterization of graphitic powders, other characterization techniques were employed for the bulk characterization. In addition to Raman spectroscopy, XPS measurements, dispersibility experiments, and IR spectroscopy were performed. However, the IR spectrum is unclear due to the high background signal of GNP (Fig. S9, ESI†).

While an increase of defects on HOPG can be detected by the appearance of a D band in Raman experiments, detection on graphitic powders is more challenging as a significant D band is already present (Fig. 2a). Additionally, the presence of other peaks (*i.e.* D\* and D') in the same region requires deconvolution of the different peaks (Fig. S6, ESI†). The heterogeneity of the graphitic powder could also cause significant differences in the observed  $I_D/I_G$  ratios complicating the analysis of the Raman results. In our experiments, the functionalized powder shows a higher  $I_D/I_G$  ratio ( $1.68 \pm 0.10$ ) in comparison to the blank GNP powder ( $1.41 \pm 0.26$ ). From this observation, we can conclude that the amount of  $sp^3$  hybridized carbon atoms is higher for the covalently functionalized materials which shows the success of the covalent grafting procedure in bulk.

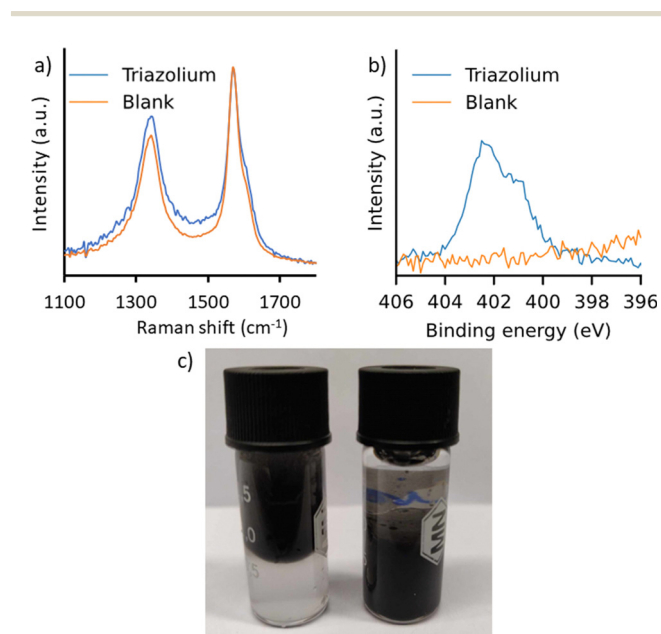


Fig. 2 Characterization of triazolium functionalized GNP by (a) Raman spectroscopy, (b) XPS nitrogen peak, and (c) dispersibility experiments of bare GNP (left) and the triazolium functionalized GNP (right) in a toluene (top)/water (bottom) mixture.

In XPS characterization of the covalently functionalized powders, a clear increase in the N content is observed, originating from the triazolium moieties that are grafted on the substrate (Fig. 2b). In the deconvolution of the nitrogen signals, different nitrogen signal contributions could be observed (Fig. S7, ESI†). A signal of positively charged nitrogen is observed at 403 eV, which arises from the nitrogen atoms at the 1 and 4 position of the triazolium. Another signal at 401 eV, with approximately half the intensity of the positively charged nitrogen, arises from the nitrogen at the 2 position of the triazolium. These signals indicate the presence of the triazolium species on the GNP substrate. From the increase in the  $N^+$  content in the XPS spectra, a catalytic loading of  $1.0 \pm 0.5 \text{ mmol g}^{-1}$  is calculated (Table S2, ESI†).

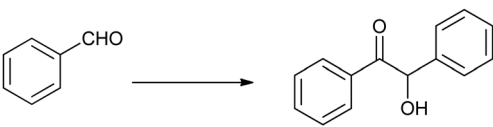
Additionally, dispersibility measurements were conducted since the attachment of charged groups (*i.e.* triazolium) to the surface should increase the hydrophilicity and thus the dispersibility of the powder in water. To determine this, the blank and functionalized powders were dispersed in a two-phase system with toluene (apolar, top layer) and water (polar, bottom layer). GNP is a strongly hydrophobic substrate that disperses in the apolar phase (Fig. 2c). However, the functionalized powder favors dispersion in the water phase showing the increased hydrophilicity of the functionalized powder.

From these characterization experiments, we conclude that the modification of graphitic substrates with NHC-precursors was successful. The next step would be to determine the catalytic activity of these functionalized substrates as organocatalysts.

The best proof of the successful functionalization of the graphitic substrate is of course its efficiency as a catalyst in commonly used reactions. For NHCs, a common reaction to test its organocatalytic activity is benzoin condensation in which two benzaldehyde moieties are coupled to form a benzoin molecule.<sup>24</sup> For this reaction, no formation of benzoin is observed when the reaction was performed in absence of GNP or in presence of the pristine GNP. However, formation of benzoin was observed when the functionalized GNP was tested as a catalyst and a yield of 17% was obtained with 3 mol% catalyst (Table 1). The functionalized powder was reused in a second run of the benzoin condensation to test its recyclability, but no formation of benzoin was observed (Table S3, ESI†). A possible explanation is the degradation of the catalyst under basic conditions *via* a  $\beta$ -elimination mechanism (Scheme S1, ESI†). The stability of both precursor 3 and precursor 5 under the basic reaction conditions were tested by stirring the precursors for 24 hours at RT, both in presence and absence of  $\text{Cs}_2\text{CO}_3$ , using 1,3,5-trimethoxybenzene as internal standard. While after stirring in absence of  $\text{Cs}_2\text{CO}_3$  the characteristic peaks could clearly be observed, these peaks disappear after stirring in basic medium (Fig. S10 and S11, ESI†). XPS and Raman characterization of the recycled powder were also performed. In the Raman experiments, similar  $I_D/I_G$  ratios were found,  $1.68 \pm 0.10$  and  $1.76 \pm 0.19$  for the functionalized and recycled powder respectively, which indicates that the grafted structure is not altered. Additionally, XPS characterization showed a significant decrease of the



**Table 1** Catalytic experiments of the functionalized powder in the benzoin condensation. Reaction conditions: 0.2 mmol benzaldehyde, 20 mol% Cs<sub>2</sub>CO<sub>3</sub>, 10 mol% 1,3,5-trimethoxybenzene (internal standard), 5 mg GNP, functionalized GNP (3 mol%) or homogeneous catalyst **5** (3 mol%), 0.5 mL THF, 24 h at RT



Powder	Yield
None (blank)	0%
GNP	0%
Funct. GNP	17%

positively charged nitrogen was observed together with a significant increase of the amine peak. This observation could suggest the removal of the triazolium species with the formation of the neutral triazole species. These experiments show the current instability of the precursor under basic conditions and further optimization of the molecular structure should be performed to inhibit degradation. Further inhibition of the degradation should lead to higher yields and recyclability of the functionalized catalysts used in this work.

In conclusion, this work reports the direct grafting of triazolium moieties on pristine carbon substrates. A thorough characterization on the nanoscale with HOPG as a model substrate allowed us to gain more insight into the nature of the functionalization. Afterward, successful upscaling to bulk graphitic materials was achieved to synthesize a covalently supported organocatalyst for benzoin condensation. The production of this material indicates the potential of covalent attachment on the graphite basal plane for the production of bulk catalysts. In follow-up experiments, the design of the catalyst and the functionalization method could be optimized to enhance the yield of the benzoin condensation reaction and the recyclability of the catalyst. Additionally, metal-based immobilized catalysts could be synthesized by using the NHC unit as a ligand. The synthesis of covalently immobilized metal-based catalysts on pristine graphitic substrates would open up a broad range of catalytic applications for these materials. Moreover, this work provides a method to combine the high control over covalent functionalization that is achieved in nanoscale experiments with bulk catalysis. When more pristine and less defected graphitic powders could be provided, the comparability of both methods would further increase which would allow more control over the catalyst design. Follow-up studies could focus on optimizing the catalytic properties of graphitic materials by combining nanoscale characterization and bulk synthesis to control the density and the location of the catalysts on the graphitic material to open up the way for designer catalysts on carbon materials.

Conceptualization: B.D., W.D., S.D.; methodology: B.D., S.B.; investigation: B.D., S.B., S.E.; supervision: W.T., W.D., S.D.;

writing – original draft: B.D.; writing – review and editing: B.D., S.B., S.E., W.T., W.D., S.D.

B. D., S. B., and S. D. F. acknowledge support from Research Foundation Flanders-FWO (I006922N, G0E3422N, GF9118N via EOS 30489208, G0H2122N via EOS 40007495), and KU Leuven – Internal Funds (C14/19/079 and C14/23/090). S. E. and W. T. thank KU Leuven (grant C14/18/061) and Research Foundation Flanders-FWO (G0A1219N) for financial support. A. Bazylevska, M. Remigio and GM Velpula are thanked for the experimental help.

## Conflicts of interest

There are no conflicts to declare.

## Notes and references

- Handbook of Heterogeneous Catalysis*, ed. G. Ertl, H. Knözinger, F. Schüth and J. Weitkamp, Wiley VCH Verlag, 2008.
- W. Wang, L. Cui, P. Sun, L. Shi, C. Yue and F. Li, *Chem. Rev.*, 2018, **118**, 9843.
- S. Sabater, J. A. Mata and E. Peris, *ACS Catal.*, 2014, **4**, 2038.
- R. Zhong, A. C. Lindhorst, F. J. Groche and F. E. Kühn, *Chem. Rev.*, 2017, **117**, 1970.
- D. M. Flanigan, F. Romanov-Michailidis, N. A. White and T. Rovis, *Chem. Rev.*, 2015, **115**, 9307.
- S. Aldroubi, N. Brun, I. Bou Malham and A. Mehdi, *Nanoscale*, 2021, **13**, 2750.
- A. Jacques, A. Devaux, C. Rubay, F. Pannetier, A. Desmecht, K. Robeyns, S. Hermans and B. Elias, *ChemCatChem*, 2023, **15**, e202201672.
- W. Zhao, Y. Tang, J. Xi and J. Kong, *Appl. Surf. Sci.*, 2015, **326**, 276.
- K. Ramesh, S. A. P. Siboro, D. W. Kim and K. T. Lim, *React. Funct. Polym.*, 2020, **152**, 104605.
- Y. Yuan, X. Wang, X. Liu, J. Qian, P. Zuo and Q. Zhuang, *Composites, Part A*, 2022, **154**, 106800.
- S. Navalon, A. Dhakshinamoorthy, M. Alvaro, M. Antonietti and H. Garcia, *Chem. Soc. Rev.*, 2017, **46**, 4501.
- B. Daelemans, N. Bilbao, W. Dehaen and S. De Feyter, *Chem. Soc. Rev.*, 2021, **50**, 2280.
- L. Lombardi, A. Kovtun, S. Mantovani, G. Bertuzzi, L. Favaretto, C. Bettini, V. Palermo, M. Melucci and M. Bandini, *Chem. – Eur. J.*, 2022, **28**, e202200333.
- K. Tahara, Y. Kubo, S. Hashimoto, T. Ishikawa, H. Kaneko, A. Brown, B. E. Hirsch, S. De Feyter and Y. Tobe, *J. Am. Chem. Soc.*, 2020, **142**, 7699.
- J. Greenwood, T. H. Phan, Y. Fujita, Z. Li, O. Ivasenko, W. Vanderlinden, H. Van Gorp, W. Frederickx, G. Lu, K. Tahara, Y. Tobe, H. Uji-I, S. F. L. Mertens and S. De Feyter, *ACS Nano*, 2015, **9**, 5520.
- M. C. Rodríguez González, A. Brown, S. Eyley, W. Thielemans, K. S. Mali and S. De Feyter, *Nanoscale*, 2020, **12**, 18782.
- H. Van Gorp, P. Walke, J. Teyssandier, B. E. Hirsch, H. Uji-I, K. Tahara, Y. Tobe, M. Van Der Auweraer and S. De Feyter, *J. Phys. Chem. C*, 2020, **124**, 1980.
- X. K. Wee, W. K. Yeo, B. Zhang, V. B. C. Tan, K. M. Lim, T. E. Tay and M. L. Go, *Bioorg. Med. Chem.*, 2009, **17**, 7562.
- D. Channe Gowda, B. Mahesh and S. Gowda, *Indian J. Chem., Sect. B: Org. Chem. Incl. Med. Chem.*, 2001, **40**, 75.
- G. B. Wang, L. F. Wang, C. Z. Li, J. Sun, G. M. Zhou and D. C. Yang, *Res. Chem. Intermed.*, 2012, **38**, 77.
- R. M. Lord, J. Holmes, F. N. Singer, A. Frith and C. E. Willans, *J. Organomet. Chem.*, 2020, **907**, 121062.
- A. Eckmann, A. Felten, A. Mishchenko, L. Britnell, R. Krupke, K. S. Novoselov and C. Casiraghi, *Nano Lett.*, 2012, **12**, 3925.
- A. Kaniyoor and S. Ramaprabhu, *AIP Adv.*, 2012, **2**, 032183.
- D. Enders, O. Niemeier and A. Henseler, *Chem. Rev.*, 2007, **107**, 5606.

